Crossing the dividing surface of transition state theory. II. Recrossing times for the atom–diatom interaction

J. C. Lorquet

Crossing the dividing surface of transition state theory. II. Recrossing times for the atom–diatom interaction

J. C. Lorquet[a]

Department of Chemistry, University of Liège, Sart-Tilman (Bâtiment B6), B-4000 Liège 1, Belgium

We consider a triatomic system with zero total angular momentum and demonstrate that, no matter how complicated the anharmonic part of the potential energy function, classical dynamics in the vicinity of a saddle point is constrained by symmetry properties. At short times and at not too high energies, recrossing dynamics is largely determined by elementary local structural parameters and thus can be described in configuration space only. Conditions for recrossing are given in the form of inequalities involving structural parameters only. Explicit expressions for recrossing times, valid for microcanonical ensembles, are shown to obey interesting regularities. In a forward reaction, when the transition state is nonlinear and tight enough, one-fourth of the trajectories are expected to recross the plane $R = R_*$ (where R_* denotes the position of the saddle point) within a short time. Another fourth of them are expected to have previously recrossed at a short negative time, i.e., close to the saddle point. These trajectories do not contribute to the reaction rate. The reactive trajectories that obey the transition state model are to be found in the remaining half. However, no conclusion can be derived for them, except that if recrossings occur, then they must either take place in the distant future or already have taken place in the remote past, i.e., far away from the saddle point. Trajectories that all cross the plane $R = R_*$ at time $t = 0$, with the same positive translational momentum P_{R_*} can be partitioned into two sets, distinguished by the parity of their initial conditions; both sets have the same average equation of motion up to and including terms cubic in time. Coordination is excellent in the vicinity of the saddle point but fades out at long (positive or negative) times, i.e., far away from the transition state. © *2014 AIP Publishing LLC*. [http://dx.doi.org/10.1063/1.4870039]

I. INTRODUCTION

The conceptual simplicity of transition state theory (TST) provides a fascinating framework for analyzing chemical reactions.[1–3] Soon after its inception by Eyring and Polanyi, Wigner[4] rooted it in firmer ground by postulating the existence of a hypersurface in phase space dividing reactants from products. The theory is then based on the assumption that all trajectories cross this surface only once and never return to it. Wigner pointed out that the optimal shape of the surface and its position should be obtained by minimizing the reactive flux, a remark that later on gave rise to variational TST.[5]

The recrossing problem has received exact and elegant solutions if the number of degrees of freedom is limited to two. First, Pollak and Pechukas[1,6] showed that the best choice of transition state (TS) in a collinear collision of an atom with a diatomic is a periodic vibration of the triatomic system. Later on, Davis and Gray[7] defined the TS as a separatrix in phase space and showed it to be always free from barrier recrossings. Unfortunately, these solutions cannot be extended to higher dimensionalities.

Closely related to the problem is the separability assumption of the reaction coordinate.[5] Experimental observations[8,9] were interpreted as evidence that, near the energy threshold, internal energy is tied up in vibrational modes orthogonal to the reaction coordinate during passage through the TS

region. This interpretation was endorsed by Marcus,[10] but was later on found to be inconsistent with quantum dynamical calculations.[11,12]

Decoupling of the reaction coordinate from a bath of oscillators for a nonseparable Hamiltonian has been the subject of intensive theoretical research. Miller exploited the dichotomy between imaginary and real frequencies to demonstrate the existence of locally conserved action variables associated with a TS even when the Hamiltonian involves a non-separable potential energy function.[13–16] Berry and Wales calculated Liapunov exponents to characterize the dynamics and presented evidence of regularity in the dynamics close to the saddle point in a systematic study of rare gas clusters[17–19] and, more recently, in more strongly coupled systems.[20,21]

The question took a new turn when Wiggins,[22–24] Komatsuzaki, Berry,[25–33] and their co-workers advocated the use of a particular system of coordinates to study the connection between decoupling and recrossing. The new set of coordinates transforms the Hamiltonian to a form containing local approximate invariants of motion even when the potential contains anharmonic terms. These normal form coordinates are nonlinear functions of both coordinates and momenta. Individual modes of the system are now defined in phase space (i.e., mixing coordinates and momenta) and there is no need to invoke, e.g., separation of time scales for their justification. At low internal energies, all of the degrees of freedom are observed to be regular and to locally maintain approximate constants of motion in the region of the TS. At higher

[a]Electronic mail: jc.lorquet@ulg.ac.be

140, 134304-1

energies, invariants of motion disappear, except that of the reactive mode,[25–30] because the latter is characterized by an imaginary frequency.[15,16] These contributions led to the definition of a dividing surface free from recrossings.

Yet, chemists are craving for a theory of reaction dynamics in configuration space, with momentum dependence reduced to a minimum.[34,35] Despite the warning that complete information cannot be obtained from theories that are based on a configuration space picture[22–24] and notwithstanding the advantages offered by the use of normal form coordinates,[22–32] we adhere in the present paper to the simplest version of TST, which reduces the dividing surface to a plane in configuration space, containing the saddle point and perpendicular to the path of steepest descent. In a trade-off between scope and simplicity, we want to know whether there exist particular cases for which recrossing of this particular surface can be approximately predicted. If dynamics can be correlated with the topography of the potential energy surface (we do not say is entirely determined by), this makes its study not only computationally simpler but also more amenable to chemical intuition.

The scope of the present contribution is necessarily restricted. The treatment is strictly classical, limited to a triatomic system, namely an atom-diatom reaction taking place in gas phase, assumes zero value for the total angular momentum and focuses attention on low internal energies.

In Sec. II, we consider a triatomic system and demonstrate the existence of symmetry properties – and therefore of dynamical constraints – in the neighborhood of a saddle point, irrespective of the shape of the potential energy function and of the internal energy. In Sec. III, a particular expression of the Hamiltonian is specified. In Sec. IV, the assumption of energy equipartition at the saddle point is shown to greatly simplify the mathematics. Recrossing times are calculated in Secs. V and VI and are shown to obey interesting regularities. In Sec. VII, the results derived by the equipartitioned model are shown to remain valid for microcanonical ensembles. Motion coordination among all degrees of freedom is studied in Sec. VIII; it is excellent in the vicinity of the saddle point but fades out at long (positive or negative) times, i.e., far away from the TS. The paper closes with a discussion, presented in Sec. IX.

II. GENERIC PROPERTIES OF THE ATOM-DIATOM INTERACTION

The Hamiltonian describing an atom-diatom interaction for a body-fixed rotationless study has been derived by several authors:[22,32,36–41]

$$H = \frac{1}{2M} P_R^2 + \frac{1}{2\mu} p_r^2 + \frac{1}{2} \left(\frac{1}{MR^2} + \frac{1}{\mu r^2} \right) p_\theta^2$$
$$+ V(R, r, \theta), \qquad (2.1)$$

where R is the distance between the atom and the center of mass of the diatomic, r the internuclear distance of the latter, θ the angle between the two position vectors, P_R, p_r, p_θ the conjugate momenta, μ the reduced mass of the diatomic, and M that of the atom–diatom system.

A closed-form expression of Hamilton's canonical equations cannot be obtained. However, local analytic solutions, valid in the neighborhood of the saddle point, can be derived as a formal series solution by repeated application of the Poisson bracket equation,[42]

$$\dot{X} = [X, H] \equiv \sum_j \left(\frac{\partial H}{\partial p_j} \frac{\partial X}{\partial q_j} - \frac{\partial H}{\partial q_j} \frac{\partial X}{\partial p_j} \right), \qquad (2.2)$$

which gives the rate of change of any dynamical variable X. Assuming initial conditions (R_0, r_0, θ_0) at time $t = 0$, the equation of motion of the reaction coordinate R can be formulated as follows:[42]

$$R(t) = R_0 + t\,[R, H]_0 + \left(\frac{t^2}{2!} \right) [[R, H], H]_0$$
$$+ \left(\frac{t^3}{3!} \right) [[[R, H], H], H]_0 + \cdots$$
$$= R_0 + c_1 t + c_2 \left(\frac{t^2}{2!} \right) + c_3 \left(\frac{t^3}{3!} \right) + \cdots, \qquad (2.3)$$

where the subscript zero refers to the initial conditions at time $t = 0$.

The first coefficients in this expansion are easily evaluated:

$$c_1 = \frac{P_{R_0}}{M}, \qquad (2.4)$$

$$c_2 = \frac{p_{\theta_0}^2}{M^2 R_0^3} - \frac{1}{M} \left. \frac{\partial V}{\partial R} \right|_0. \qquad (2.5)$$

Now, assume that the potential energy surface is characterized by a saddle point at coordinates (R_*, r_*, θ_*) and consider a bundle of 16 forward trajectories that all begin at time $t = 0$ at $R_0 = R_*$, with the same translational momentum normal to the dividing surface denoted $P_{R_0} = P_{R_*}$, and with the 16 possible sign combinations in the set $\{r_* \pm \delta r, \pm p_{r_0}, \theta_* \pm \delta\theta, \pm p_{\theta_0}\}$ for the other variables. As discussed in detail in Paper I,[41] it is advantageous to split this bundle into two sets of eight trajectories. The set having an even number of minus signs in the specification of their initial conditions is denoted as *gerade*. The remaining eight trajectories form the *ungerade* set. This distinction makes it possible to derive symmetry properties for coefficients c_2 and c_3 that are valid irrespective of the expression of the potential energy function $V(R, r, \theta)$. Symmetry induces constraints on the trajectories and will be shown in what follows to have implications for the dynamics on both sides of the time origin, namely local regularity in the neighborhood of a saddle point.

First, note that the coefficient c_2, which determines the acceleration of the translational motion along the reaction coordinate, depends neither on p_r, nor on the sign of p_θ. Therefore, at very short times, trajectories are the same for the four states $\{\pm p_{r_0}, \pm p_{\theta_0}\}$. In other words, under the influence of the quadratic term, the bundle splits into four sets of four trajectories having the same translational motion.

The role of the coefficient c_3 is to further split the bundle into 16 individual trajectories at later times. However, as shown in Paper I,[41] the average value of c_3 is observed to be the same for the two sets: $\langle c_3 \rangle_g = \langle c_3 \rangle_u$. Unfortunately, the

expression of the coefficient c_4 is very complicated and no regularity could be discerned. As a consequence, *gerade* and *ungerade* trajectories have the same average equation of motion, up to and including terms cubic in time,

$$\langle R(t)\rangle_g = \langle R(t)\rangle_u + O(t^4) + \cdots. \qquad (2.7)$$

A similar relation is also valid for the other two coordinates, r and θ, and for their conjugate momenta.

Summing up, Eq. (2.1) provides a Hamiltonian with a completely general potential part, which generates trajectories that are necessarily constrained by regularities and symmetries in the neighborhood of a saddle point.

In principle, the derivation of symmetry properties for the coefficients c_2 and c_3 is valid at any energy. However, the concept of average trajectories makes sense only if the 16 initial points have at least comparable energies. This will be the case if the anharmonicity of the vibrational and angular motions is weak and if the elongations δr and $\delta\theta$ are not too great, i.e., if the energy is not too high. Therefore, the concept of a bundle of 16 closely related trajectories is particularly relevant at low energies only. Note, however, that a certain range of tolerance for the energy is acceptable because inherent in the definition of microcanonical ensembles. This point will be discussed in Sec. VII.

To get further insight and more detailed information, it is necessary to specify the expression of the potential energy surface.

III. A SPECIFIC HAMILTONIAN

After examination of several possible expressions of the potential energy function, it was found most efficient to follow the proposals of Murrell and co-workers[43,44] and of Green *et al.*[20] Specifically, the potential is written as a sum of two- and three-body contributions, adopting the simplest possible expression for the two-body terms (in contrast to previous attempts[45]), and shifting most of the couplings to the three-body term:

$$V(R, r, \theta) = V_{saddle}(R) + V_{diat}(r, R)$$
$$+ V_{ang}(\theta, R) + V_{3b}(R, r, \theta). \qquad (3.1)$$

A. Reaction coordinate

The first term of this expansion, representing a cross-section along the reaction coordinate, is written as an inverted 6–12 Lennard-Jones potential where the zero of energy has been shifted to the saddle point and in which the length-scale parameter σ has been replaced by the position of the saddle point, denoted R_*. It can be written either as

$$V_{saddle}(R) = -\Delta E \left(1 - \left(\frac{R_*}{R}\right)^6\right)^2, \qquad (3.2)$$

where ΔE denotes the reverse activation energy barrier, or as

$$V_{saddle}(R) = -\frac{M\, R_*^2 \Omega^2}{72} \left(1 - \left(\frac{R_*}{R}\right)^6\right)^2, \qquad (3.3)$$

where Ω denotes the modulus of the imaginary frequency. The use of Eq. (3.3) is preferable, because entirely defined in terms of the local properties of the potential energy surface in the neighborhood of the saddle point, whereas Eq. (3.2) depends on how well the long-range $-R^{-6}$ potential fits the actual surface. Both parameterizations assume the same general shape as an inverted Morse potential where the decreasing exponential is replaced by a $(R_*/R)^6$ function. The decrease in potential energy is sharp on one side of the saddle point and gentle on the other.

The developments that follow are thus restricted to reactions with a strongly asymmetric reaction profile, presenting a steep increase on the left of the TS and a smooth $-R^{-6}$ asymptotic decrease at larger internuclear separations. It is therefore necessary to distinguish two cases in the applications that follow. If one wishes to study the last TS in a unimolecular dissociation or the exit channel in an endothermic bimolecular reaction, then Eqs. (3.2) or (3.3) should be used with initial conditions $R_0 = R_*$ and $P_{R_0} = + P_{R_*}$. These processes will be referred to as forward reactions. Alternatively, exothermic bimolecular reactions with an activation energy barrier in the entrance channel or recombination reactions seen as the inverse of a unimolecular dissociation will be referred to as backward reactions, for which the appropriate initial conditions are $R_0 = R_*$ and $P_{R_0} = - P_{R_*}$.

B. Vibration of the diatomic

The next two-body term describes the vibrational motion of the diatomic fragment. To introduce anharmonicity in a simple way, a Simons-Parr-Finlan potential is used.[40,46] Furthermore, curvature of the reaction path is introduced by allowing the frequency and equilibrium distance of the diatomic fragment to depend on the reaction coordinate R. Altogether,

$$V_{diat}(r, R) = \frac{1}{2}\mu\omega(R)^2(r - r_{eq}(R))^2 \left(\frac{r_{eq}(R)}{r}\right)^2 \qquad (3.4)$$

with

$$r_{eq}(R) = r_\infty + (r_* - r_\infty)\left(\frac{R_*}{R}\right)^6, \qquad (3.5)$$

$$\omega(R) = \omega_\infty + (\omega_* - \omega_\infty)\left(\frac{R_*}{R}\right)^6, \qquad (3.6)$$

where r_∞ and ω_∞ denote the equilibrium distance and angular frequency of the diatomic fragment after complete separation, respectively. The inverse sixth power dependence is in line with the assumption of an inverse Lennard-Jones potential for the reaction coordinate.

C. Angular degree of freedom

Angles are measured so that the equilibrium value at the saddle point, denoted θ_*, is positive and tends to zero as R increases. The potential that determines the angular motion, which is a hindered rotation with a strongly R-dependent barrier, is written as

$$V_{ang}(\theta, R) = V_0 \left(\frac{R_*}{R}\right)^6 \sin^2(\theta - \theta_{eq}(R)), \qquad (3.7)$$

with

$$\theta_{eq}(R) = \theta_* \left(\frac{R_*}{R} \right)^6 . \tag{3.8}$$

At low energies, the motion resembles that of a harmonic oscillator having a frequency equal to[47]

$$\nu = \frac{1}{\pi} \sqrt{\frac{V_0}{2 I_*}}, \tag{3.9}$$

where I_* denotes the reduced moment of inertia

$$I_* = \left(\frac{1}{M R_*^2} + \frac{1}{\mu r_*^2} \right)^{-1} . \tag{3.10}$$

D. Three-body interaction term

To derive the expression of the last term of the potential, we adapt Murrell's procedure to a saddle point topography described in Jacobi coordinates. The three-body term is written as a polynomial in the three coordinates R, r, θ, multiplied by the product of two "range functions:"[43,44] first, a standard Sorbie-Murrell hyperbolic tangent function for the vibrational coordinates r and a second one for the translational coordinate R.

The expression of the polynomial and that of the range function appropriate to motion across a saddle point are determined from the following requirements.[44] First, V_{3b} should tend asymptotically to zero at large values of R. Second, its Taylor expansion about the saddle point should not contain linear terms. Third, it should change its sign as the saddle point region is crossed. (Otherwise, the interaction would be the same at $R = R_* + dR$ and at $R = R_* - dR$, which is illogical). It results from these requirements that the polynomial should start with quadratic terms. The three-body interaction term is therefore written as

$$V_{3b}(R, r, \theta) = P(R, r, \theta) \left(\frac{R_*}{R} \right)^6 \left(1 - \left(\frac{R_*}{R} \right)^6 \right)$$

$$\times \left(1 - \tanh \left(\frac{\gamma}{2} (r - r_{eq}(R)) \right) \right), \tag{3.11}$$

with

$$P(R, r, \theta) = \beta_{RR}(R - R_*)^2 + \beta_{rr}(r - r_*)^2 + \beta_{\theta\theta}(\theta - \theta_*)^2$$
$$+ \beta_{Rr}(R - R_*)(r - r_*) + \beta_{R\theta}(R - R_*)(\theta - \theta_*)$$
$$+ \beta_{r\theta}(r - r_*)(\theta - \theta_*). \tag{3.12}$$

Including only quadratic terms in the expansion of the three-body interaction restricts the accuracy in the space domain and therefore confines the validity of the laws of motion to a limited range of time. Additional terms would certainly be necessary to describe the dynamics at short R distances since anharmonic couplings increase strongly in this region. On the other hand, as pointed out by Murrell, a high-order polynomial P is likely to induce spurious stationary points in the potential energy surface. It has been checked that the use of Eq. (3.11), with Eq. (3.12) truncated as it is, makes it possible to describe shallow basins resulting, e.g., from the presence of van der Waals complexes in the exit channel of the reaction.

Clearly, not all reactive processes can be studied with this Hamiltonian. Recent research[20,21,45] has shown that reaction dynamics is highly sensitive to the topography of the saddle point region. Results derived for the strongly asymmetric steepest-descent paths considered here would not be valid for smoother reaction profiles found, e.g., in isomerization reactions of rare gas clusters.[17–21,45] Furthermore, so-called non-RRKM reactions[11,12,48] and roaming pathways[49–51] are outside its scope. Nevertheless, we believe it to be realistic enough to identify general trends in short-time dynamics in many cases.

IV. ENERGY EQUIPARTITION

To derive the equations of motion from Eq. (2.3) (and similar ones for the other degrees of freedom) for the 16 trajectories mentioned in Sec. II, it is necessary to specify the initial conditions.

Energy randomization at the saddle point is a common assumption in theories of chemical reactivity. During its previous history before reaching the TS, the system usually evolves under the influence of a strongly anharmonic potential energy function. Complications in the reaction path and nonlinearities in the force field are expected to lead to rapid energy transfer among the vibrational degrees of freedom leading to a microcanonical distribution. This possibility is strengthened by the fact that the molecular system usually receives its internal energy from a nonspecific random process, i.e., most of the time by thermal excitation. However, phase space may be metrically decomposable and warnings against the blind use of this assumption have been issued, e.g., by Hase and co-workers.[11,12,48]

The position adopted here is to consider the situation where the internal energy is shared equally among all of its components at the saddle point as a convenient reference point that, as will be described in Secs. V and VI, greatly simplifies the mathematics. At a later stage, in Sec. VII, it will be shown that the derived results remain valid for systems that are not equipartitioned but that are in microcanonical equilibrium.

For now, attention is restricted to a subset of trajectories for which we assume, based on Eqs. (2.1), (3.1), and (3.4)–(3.8),

$$\frac{1}{2 M} P_{R_*}^2 = \frac{1}{2 \mu} p_{r_*}^2 = \frac{1}{2 I_*} p_{\theta_*}^2 = \frac{1}{2} \mu \, \omega_*^2 \, \delta r_*^2 = V_0 \sin^2 \, \delta\theta_*, \tag{4.1}$$

where δr_*, $\delta\theta_*$, p_{r_*}, and p_{θ_*} denote the moduli of initial elongations that satisfy energy equipartition. The latter quantities are now expressed in terms of the modulus of the translational momentum P_{R_*}. Each momentum and each elongation can be positive or negative and its modulus is listed below:

$$p_{r_*} = \sqrt{\frac{\mu}{M}} |P_{R_*}|, \tag{4.2}$$

$$\delta r_* = \frac{|P_{R_*}|}{\sqrt{M \mu} \, \omega_*}, \tag{4.3}$$

$$p_{\theta_*} = \left(\frac{I_*}{M} \right)^{1/2} |P_{R_*}|, \tag{4.4}$$

$$\delta\theta_* = \arcsin\left(\frac{|P_{R_*}|}{\sqrt{2\,M\,V_0}}\right). \qquad (4.5)$$

The 16 trajectories are generated by the 16 possible sign combinations assumed for these momenta and elongations. Due to the dependence of the centrifugal energy on r, the 16 initial states are not degenerate at the saddle point. They split into two groups of 8 states, one characterized by initial vibrational coordinates equal to $r_* + \delta r_*$, and to $r_* - \delta r_*$ for the other. However, the energy difference between the two groups is small, at least at low energies. The ratio between the energy gap and the average energy of the two sets is calculated to be of the order of $\delta r_* / r_*$, which is tolerably small in an ensemble average.

V. AVERAGE RECROSSING TIMES

A. The cubic approximation

The formal series solution, Eq. (2.3), has several severe shortcomings. It converges poorly and it is impractical to include many terms because their complexity increases tremendously rapidly with their order. Furthermore, even when it can be calculated, the resulting high-order polynomial uses its flexibility to scrupulously fit the trajectory near its origin at $t = 0$, including insignificant irregularities if any, and is a poor extrapolation function to predict the long-time behavior. However, if interest is focused on short-time dynamics, then truncation after the cubic term may provide reliable results. This limits our study to the prediction of rapid recrossings, taking place in the near future, or to the detection of those that have already taken place at negative times, but in a recent past. As a final justification, we note that a short-time approximation is in the spirit of TST, which aims at linking reactivity to the properties of a restricted range of the potential energy surface in the immediate neighborhood of its saddle point.

Recall the conclusions of Sec. II. At very short times, the bundle of 16 trajectories splits into four sets of four trajectories having the same translational motion. Each set is characterized by a particular initial value of the spatial (i.e., vibrational and angular) coordinates, r_0 and θ_0, and consists of four trajectories corresponding to the four possible sign combinations for the conjugate momenta $\{\pm p_{r_0}, \pm p_{\theta_0}\}$. The role of the coefficient c_3 is to further split the bundle into 16 individual trajectories at later times.

We now define an average trajectory for each one of the four sets, and determine its recrossing time by calculating the roots of the following equation:

$$R(t) = R_* + \frac{P_{R_0}}{M}t + \frac{1}{2}\langle c_2\rangle t^2 + \frac{1}{6}\langle c_3\rangle t^3 = R_*, \qquad (5.1)$$

where $\langle c_2\rangle$ and $\langle c_3\rangle$ denote the averages of the quadratic and cubic terms over the four possible sign combinations $\{\pm p_{r_0}, \pm p_{\theta_0}\}$. (Note, however, that the recrossing time of this average trajectory is not necessarily the same as the average of the recrossing times of each individual trajectory.) Equation (5.1) transforms into

$$\frac{P_{R_0}}{M} + \frac{1}{2}\langle c_2\rangle t + \frac{1}{6}\langle c_3\rangle t^2 = 0. \qquad (5.2)$$

The short-time cubic approximation will be reliable only if the two roots of Eq. (5.2) satisfy a number of requirements. One root should be positive, the other should be negative. Only that with the smallest modulus is deemed reliable. To go further into the analysis, it is necessary to remember that, as explained in Sec. III, one should distinguish between two kinds of reactive processes, namely forward reactions with a positive value of the initial translational momentum $P_{R_0} = +P_{R_*}$ and reverse reactions where this momentum is negative. Estimates of recrossing times will be reliable only if the magnitude of $\langle c_2\rangle$ and $\langle c_3\rangle$ falls within a certain range.

To make the equations that follow easier to read, we put

$$x = \sqrt{\mu}\,\omega_*\,(r_* - r_\infty), \qquad (5.3)$$

$$y = \sqrt{2\,V_0}\,\theta_*, \qquad (5.4)$$

$$z = \sqrt{M}\,\Omega\,R_*, \qquad (5.5)$$

$$u = 36\,x^2 + 36\,y^2 - z^2, \qquad (5.6)$$

$$f(p, q\,;\, m, n) = p\,(m\,x^2 + n\,x\,y + m\,y^2) - q\,z^2. \qquad (5.7)$$

When Eq. (5.2) is rewritten in terms of these new variables and when the assumption of energy equipartition is introduced, average recrossing times can be obtained as a series expansion in P_{R_*}. The results differ for forward and reverse reactions and are now analyzed in each case.

B. Forward reactions

Consider unimolecular dissociations or endothermic bimolecular reactions. In that case, the fragments escape from a deep well, overcome a barrier, and follow their course under the influence of a $-R^{-6}$ potential. The appropriate initial conditions are $R_0 = R_*$ and $P_{R_0} = +P_{R_*}$.

1. The first set of initial conditions

Let us start with the first set, consisting of four trajectories with initial conditions for the spatial elongations equal to $r_* + \delta r_*$, and $\theta_* + \delta\theta_*$, where δr_* and $\delta\theta_*$ are defined as positive quantities determined by energy equipartition, i.e., are given by Eqs. (4.3) and (4.5). The recrossing time of the average of these four trajectories is obtained by calculating the roots of Eq. (5.2). The root having the smallest modulus is equal to

$$\langle\tau^{fwd}\rangle = \langle\tau^{fwd}\rangle_0 + \frac{3}{2}\frac{P_{R_*}R_*}{u}\,F^{fwd}(x, y, z) + O(P_{R_*}^2), \qquad (5.8)$$

with

$$\langle\tau^{fwd}\rangle_0 = \frac{6\sqrt{M}\,R_*}{9\,(x + y) + \sqrt{3}\,f(9, 2\,;\,11, 6)^{1/2}} \qquad (5.9)$$

and

$$F^{fwd}(x, y, z)$$

$$= 3 - \sqrt{3}\left(37x + 144\left(1 - \frac{r_\infty}{r_*}\right)x + 96\left(1 - \frac{\omega_\infty}{\omega_*}\right)x + 85y - 4\sqrt{\frac{2}{V_0}}\beta_{R\theta}R_* - 8\frac{\beta_{Rr}R_*}{\sqrt{\mu}\,\omega_*}\right)f(9, 2; 11, 6)^{-1/2}$$

$$- 6\left(\frac{\beta_{rr}}{\mu\,\omega_*^2} + \frac{\beta_{\theta\theta}}{2V_0} + \frac{\beta_{R\theta}}{\sqrt{2}\sqrt{V_0}\sqrt{\mu}\,\omega_*}\right)(1 - 3\sqrt{3}\,(x + y)\,f(9, 2; 11, 6)^{-1/2})$$

$$+ 24\left(7x + 36\left(1 - \frac{r_\infty}{r_*}\right)x + 24\left(1 - \frac{\omega_\infty}{\omega_*}\right)x + 19y - \sqrt{\frac{2}{V_0}}\beta_{R\theta}R_* - 2\frac{\beta_{Rr}R_*}{\sqrt{\mu}\,\omega_*}\right)$$

$$\times (9x + 9y + \sqrt{3}\,f(9, 2; 11, 6)^{1/2})^{-1}. \tag{5.10}$$

At very low energies, Eq. (5.9) provides a good approximation to the recrossing time. The role of the function F is to provide a correction when energy is increased. Its daunting appearance supports the view that TST is essentially a low-energy theory.

Inspection of Eqs. (5.2) (when written explicitly), (5.9), and (5.10) shows that recrossings will be rapid (and hence reliably predicted) if two conditions are fulfilled:

$$x + y \gg \frac{P_{R_*}}{\sqrt{M}}, \tag{5.11}$$

$$z \ll 6(x^2 + y^2)^{1/2}. \tag{5.12}$$

The physical significance of these conditions will be specified shortly.

A particularly interesting situation is the limiting case corresponding to very low energies. When P_{R_*} is vanishingly small, the recrossing time of the average of the four trajectories defined by the first set of initial conditions is equal to $\langle\tau^{fwd}\rangle_0$. Interestingly enough, it depends on structural parameters only, namely, M, μ, R_*, r_*, r_∞, Ω, ω_*, θ_*, and V_0. We mention, for its simplicity and for the insight it provides, an approximation which is valid if inequalities (5.11) and (5.12) are obeyed, i.e., if the structure of the TS is sufficiently different from that of the products (which amounts to requiring that it be tight enough), with x and y having similar orders of magnitude, a condition that excludes, e.g., linear TSs (for which $\theta_* \approx 0$):

$$\langle\tau^{fwd}\rangle_0 \approx \frac{\sqrt{M}\,R_*}{4(x + y)}. \tag{5.13}$$

At this juncture, it proves convenient to introduce a distinction based on the relative stiffness or softness of the oscillator in the TS and in the separated fragment and to distinguish two subcases. If $\omega_* < \omega_\infty$, with, as a natural consequence, $r_* > r_\infty$ and hence $x > 0$, the TS will be termed soft. Conversely, in a stiff TS, $\omega_* > \omega_\infty$, $r_* < r_\infty$, and $x < 0$. This distinction should not be confused with the dichotomy between tight and loose TSs. (In the present paper, a loose TS is defined by the requirements $r_* \approx r_\infty$ and $\theta_* \approx 0$, i.e., a nearly collinear geometry and similar bond distances in the TS and

in the separated fragments, irrespective of the magnitude of the reverse activation energy barrier.)

This distinction is useful in the discussion of recrossing times. If the TS is soft, i.e., if x is positive, then the denominator of Eq. (5.9) consists of a sum of three positive quantities, because θ_* and thus y are always positive by definition. The zero-energy recrossing time $\langle\tau^{fwd}\rangle_0$ of the average trajectory is then necessarily positive. It will furthermore be small, i.e., reliably predicted, if the TS is tight enough, i.e., if x and y are large enough and z small enough. The average trajectory is then predicted to recross in the near future.

However, if the TS is stiff, x is negative, and Eqs. (5.9) and (5.13) generate a large and hence unreliable estimate of the recrossing time $\langle\tau^{fwd}\rangle_0$. In other words, the cubic approximation is unable to provide any reliable prediction for the first set of initial conditions if the TS is stiff. This means that one must remain noncommittal: recrossings are possible but uncertain and are shifted to an unpredictable distant future or remote past.

To complete the discussion in terms of structural parameters, it is useful to derive the physical significance of parameter z, which is obtained by comparing Eqs. (3.2) and (3.3),

$$z = \sqrt{M}\,\Omega\,R_* = 6\sqrt{2\,\Delta E}. \tag{5.14}$$

In plain language, this analysis shows that, in a forward reaction, the tighter the TS (in the sense just defined), the lower the reverse activation energy barrier, the more rapidly the recrossing will take place. The first set of four trajectories then does not contribute to the reaction rate.

At higher energies, the whole set of Eqs. (5.8)–(5.10) must be used. Average recrossing times now vary with the internal energy and depend on coupling constants. This result supports the conclusion derived by Berry, Komatsuzaki, and Wales[18, 25, 26, 28, 30] who distinguish three successive regimes in the local dynamics as the internal energy is increased: first, quasiregular, then intermediate semichaotic, and finally stochastic.

2. The second set of initial conditions

In a similar way, the second set consists of four trajectories that are all characterized by the same initial conditions

for the vibrational and angular variables, namely $r_0 = r_* - \delta r_*$ and $\theta_0 = \theta_* - \delta \theta_*$. The recrossing time of the average of these four trajectories is again obtained by calculating the roots of Eq. (5.2) with these initial conditions. The one with the smallest modulus is given by equations that are the same as those derived for the first set, except that Eq. (5.9) is now replaced by its opposite, namely

$$\langle \tau^{fwd} \rangle_0 = -\frac{6\sqrt{M}\,R_*}{9\,(x+y) + \sqrt{3}\,f(9,\,2\,;11,\,6)^{1/2}}. \tag{5.15}$$

Therefore, if the TS is soft and the energy in excess of the saddle point very low, one concludes that, before crossing the dividing surface at time $t = 0$, the average trajectory has already recrossed in the recent past because it had its origin in the fragment space. This conclusion can be expected to remain qualitatively valid at slightly higher energies, although Eqs. (5.8)–(5.10) should be used in full. The second set of four trajectories thus does not contribute either to the reaction rate. If the TS is stiff, no reliable conclusion can be derived.

3. The remaining two sets of initial conditions

The remaining two sets of trajectories are similarly treated. They now lead to recrossing predictions that are reliable for stiff TSs only. No conclusion can be derived for soft TSs. The equations that determine recrossing times are easily derived from the previous one, simply by replacing x by $-x$, β_{Rr} by $-\beta_{Rr}$, and $\beta_{r\theta}$ by $-\beta_{r\theta}$.

The initial conditions of the four trajectories of the third set are $r_0 = r_* - \delta r_*$, and $\theta_0 = \theta_* + \delta \theta_*$. The predictions are entirely analogous to those derived for the first set, except that they now concern stiff TSs. The recrossing time of the average trajectory is predicted to take place in the near future.

The fourth set consists of four trajectories whose initial conditions $r_0 = r_* + \delta r_*$ and $\theta_0 = \theta_* - \delta \theta_*$. The situation is now analogous to that of the second set. If the TS is stiff, then the average trajectory is predicted to have previously recrossed in the recent past.

4. Conclusions

In sum, whatever the soft or stiff nature of a TS, all of the information on the recrossing times that can be derived in a reliable way can be summarized by saying that there exist four trajectories that can be expected to recross at times of the order of $\langle \tau^{fwd} \rangle_0$ and four trajectories that have previously recrossed at negative times approximately equal to $-\langle \tau^{fwd} \rangle_0$. These eight trajectories do not contribute to the reaction rate. No reliable information can be derived on the fate of the remaining eight trajectories.

5. Numerical example

Classical trajectories have been calculated for the formyl radical decomposition reaction $HCO \rightarrow H + CO$ by numerical integration of Hamilton's canonical equations. The assumed potential energy surface is that derived by Cho *et al.*[52] with one modification. The calculated structure of the TS
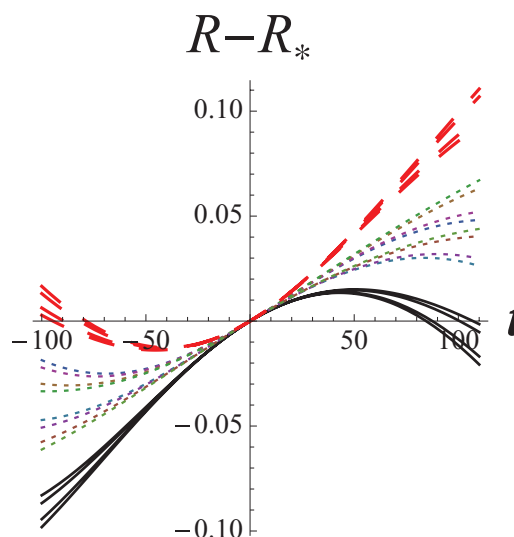

FIG. 1. Classical trajectories for the reaction $HCO \rightarrow H + CO$ calculated by numerical integration of Hamilton's canonical equations. Out of the bundle of 16 trajectories, four (black lines) start in the reactant space, cross the dividing surface at $t = 0$, and rapidly return to it; four (dashed red lines) have their origin in the product space, cross the dividing surface at a negative time, recross at $t = 0$ and head for infinity; the fate of the remaining eight trajectories (dotted lines) is uncertain. Time and distances in atomic units.

does not fulfill the conditions expressed in Eqs. (5.11) and (5.12). Therefore, we made it tighter by assuming a T-shaped structure ($\theta_* = 90°$). Furthermore, the CO bond distance in the TS, r_*, has been increased (from 1.15 Å to 1.25 Å). All other structural parameters were unchanged. The values of the coupling constants β_{ij} (Eq. (3.12)) have been chosen large enough to generate conspicuous changes in the potential energy surface but not enough to introduce spurious energy barriers. Trajectories have been calculated with initial conditions corresponding to an energy of 1 kcal/mole above the saddle point.

The graph representing the motion along the reaction coordinate is given in Fig. 1. Clearly, four trajectories have their origin in the product space, temporarily cross to the bound space at a short negative time, and recross again at $t = 0$. Four others start in the reactant space, cross the dividing surface at $t = 0$, and rapidly return to it. The Pechukas characteristic function[1] χ is equal to zero for these two sets. The remaining eight trajectories cross only once in the studied time range, but their fate in the remote past or future is indeterminate and cannot be analytically ascertained in the cubic approximation. Reactive trajectories are to be sought among them.

Average trajectories have not been drawn to avoid cluttering. The recrossing times calculated by numerical integration are $+95$ a.u. and -86 a.u. (i.e., $+2.3$ or -2.1 femtoseconds) for the first and second sets, respectively. The analytical recrossing times $\langle \tau^{fwd} \rangle$ derived from Eq. (5.8) are $+85$ a.u. and -76 a.u., whereas the zero-energy approximation $\langle \tau^{fwd} \rangle_0$ predicts $+79$ a.u. (Eq. (5.9)), -79 a.u. (Eq. (5.15)), and $+75$ a.u. (Eq. (5.13)). The discrepancy between analytical and numerical estimates results from the use of the cubic approximation and from the truncation to first order of the series expansion in P_{R_*}.

For the first group of trajectories, the maximum elongation beyond the dividing surface before returning to it is of the order of 0.015 a.u. = 0.008 Å.

Clearly, the present method is limited to a semi-quantitative study of short-time dynamics, i.e., of the immediate neighborhood of the TS. It is, however, interesting to note that there exist cases where, after a couple of femtoseconds, one half of the trajectories have to be discarded as nonreactive.

C. Reverse reactions

We now consider the case of an exothermic bimolecular reaction with an activation energy barrier in the entrance channel, at large values of R, after which the potential falls off steeply into the exit valley, or a recombination reaction seen as the inverse of a unimolecular dissociation. The appropriate initial conditions are now $R_0 = R_*$ and $P_{R_0} = -P_{R_*}$.

Here, we start with the set consisting of four trajectories with initial conditions for the spatial elongations equal to $r_* - \delta r_*$ and $\theta_* - \delta \theta_*$ (where δr_* and $\delta \theta_*$ are defined as positive quantities given by Eqs. (4.3) and (4.5)).

The shortest recrossing time of the average of these four trajectories is equal to

$$\langle \tau^{rev} \rangle = \langle \tau^{rev} \rangle_0 + \frac{3}{2} \frac{P_{R_*} R_*}{u} F^{rev}(x, y, z) + O\left(P_{R_*}^2\right) \tag{5.16}$$

with

$$\langle \tau^{rev} \rangle_0 = \frac{6\sqrt{M} R_*}{9(x+y) + \sqrt{3} f(-9, -2; 5, -6)^{1/2}} \tag{5.17}$$

and

$$
\begin{aligned}
&F^{rev}(x, y, z) \\
&= 3 + \sqrt{3}\left(19x + 144\left(1 - \frac{r_\infty}{r_*}\right)x + 96\left(1 - \frac{\omega_\infty}{\omega_*}\right)x + 67y - 4\sqrt{\frac{2}{V_0}}\beta_{R\theta} R_* - 8\frac{\beta_{Rr} R_*}{\sqrt{\mu}\,\omega_*}\right) f(-9, -2; 5, -6)^{-1/2} \\
&\quad - 6\left(\frac{\beta_{rr}}{\mu\,\omega_*^2} + \frac{\beta_{\theta\theta}}{2V_0} + \frac{\beta_{r\theta}}{\sqrt{2}\sqrt{V_0}\sqrt{\mu}\,\omega_*}\right)\left(1 - 3\sqrt{3}(x+y) f(-9, -2; 5, -6)^{-1/2}\right) \\
&\quad - 24\left(7x + 36\left(1 - \frac{r_\infty}{r_*}\right)x + 24\left(1 - \frac{\omega_\infty}{\omega_*}\right)x + 19y - \sqrt{\frac{2}{V_0}}\beta_{R\theta} R_* - 2\frac{\beta_{Rr} R_*}{\sqrt{\mu}\,\omega_*}\right) \\
&\quad \times (9x + 9y + \sqrt{3} f(-9, -2; 5, -6)^{1/2})^{-1}.
\end{aligned}
\tag{5.18}
$$

The conditions for recrossings to be rapid in a reverse reaction are, as before, derived from an analysis of Eqs. (5.2), (5.16), and (5.17). The inequality expressed in Eq. (5.11) is again required and, here again, the TS is required to be tight. However, Eq. (5.12) is now replaced by its opposite:

$$z \gg 6(x^2 + y^2)^{1/2}. \tag{5.19}$$

The latter condition, together with the requirement that x and y be large enough can be fulfilled only if the activation energy barrier is very large, as shown by Eq. (5.14). However, a high value of this barrier is contradictory with the spirit of our model where the parameterization as an inverse Lennard-Jones potential with its smooth $-R^{-6}$ decrease (Eq. (3.2)) is appropriate for small barriers only. Hence, we will limit ourselves to the statement that, in reverse reactions, recrossings are impossible for flat saddles and small activation energy barriers.

VI. INDIVIDUAL RECROSSING TIMES AT LOW ENERGIES

The concept of average trajectory only makes sense if the dispersion (i.e., the difference between the largest and smallest values of the recrossing times) is not too large. Therefore,

we evaluate the individual recrossing times of each trajectory in each set. Manageable formulas can be derived at vanishingly small energies only. For reasons explained in paragraph VC, we limit ourselves to the study of forward reactions.

A. Forward reactions for a soft TS

Reliable information on fast recrossings can be derived for the four trajectories of the first set, having initial conditions for the spatial elongations equal to $r_* + \delta r_*$ and $\theta_* + \delta \theta_*$. They are found to recross at positive times given by the four possible sign combinations of the following expression:

$$\tau_{soft}^{fwd} = \langle \tau^{fwd} \rangle_0 + A^{fwd}\left(\pm \omega_* x \pm 2\frac{V_0 \theta_*}{\sqrt{I}}\right), \tag{6.1}$$

with $\langle \tau^{fwd} \rangle_0$ given by Eq. (5.9) and

$$A^{fwd} = 6\frac{M R_*^2}{u^2}\left(9x + 9y - \frac{\sqrt{3} f(9, 1; 7, 6)}{f(9, 2; 11, 6)^{1/2}}\right), \tag{6.2}$$

A^{fwd} being a negative quantity. Equation (6.1) is easily rewritten as

$$\tau_{soft}^{fwd} = \langle \tau^{fwd} \rangle_0 \pm \Delta\tau^{vib} \pm \Delta\tau^{ang}. \tag{6.3}$$

The individual recrossing times of each of the four trajectories at vanishingly low energies are symmetrically located on either side of the average value $\langle \tau^{fwd} \rangle_0$. The shortest (and most reliably predicted) recrossing time is observed for the trajectory having $\{+p_{r_*}, +p_{\theta_*}\}$ as initial conditions because the two signs that occur in Eq. (6.1) are then positive. A symmetric pair of intermediate recrossing times is generated when the vibrational and angular momenta have different signs. The trajectory having $\{-p_{r_*}, -p_{\theta_*}\}$ as initial conditions is predicted to be the last one to recross. However, this prediction is the least reliable: because of the increasing influence of the quartic and higher terms, one might end up with a near miss although the cubic approximation predicts a genuine recrossing.

The four trajectories of the second set, with initial conditions given by $r_* - \delta r_*$ and $\theta_* - \delta \theta_*$, are expected to recross at negative times, which are given by equations similar to Eqs. (6.1) and (6.3) where the first term of the right-hand side is now $-\langle \tau^{fwd} \rangle_0$. In other words, these four trajectories had their origin in the product state.

B. Forward reactions when the TS is stiff

The equations that determine recrossing times are easily derived from those valid in the soft case, simply by replacing x by $-x$. The four trajectories having initial conditions for spatial elongations equal to $r_* - \delta r_*$ and $\theta_* + \delta \theta_*$ are found to recross at four positive times positioned in a symmetrical pattern around the recrossing time of the average trajectory. The same is true for the last set, with initial conditions given by $r_* + \delta r_*$ and $\theta_* - \delta \theta_*$; the four recrossing times are arranged symmetrically around a negative average time.

C. Conclusions

In summary, assuming not too high energies, if inequalities (5.11) and (5.12) are fulfilled, whatever the softness or stiffness of the TS, out of the 16 trajectories of the bundle there will always be a set of four trajectories whose average recrosses the dividing surface at a small positive time in the near future and thus returns to the reactant space. There will be another set of four trajectories whose average has already recrossed in the recent past, coming from the reactant space and returning to it. These trajectories do not contribute to the reaction rate.

If the energy is low, the eight trajectories that do not contribute to the reaction rate are observed to recross or to already have recrossed at the eight times given by the eight possible sign choices in an equation having the form

$$\tau^{fwd} = \pm \langle \tau^{fwd} \rangle_0 \pm \Delta \tau^{vib} \pm \Delta \tau^{ang}. \qquad (6.4)$$

The complete list of predictions derived from a first-order expansion in P_{R_*} is given in Table I. The numerical example presented in Fig. 1 illustrates these conclusions. A number of points should be noted.

Inspection of Table I shows that rapid recrossings are induced by a large amount of potential energy in the spatial degrees of freedom; they require the vibrational coordinate to be strongly stretched with respect to its asymptotic value (i.e., when $r_0 > r_* > r_\infty$ if the TS is soft or when $r_0 < r_* < r_\infty$ if the TS is stiff) with, in addition, $\theta_0 > \theta_* > 0$ in both cases. Recrossings are thus induced by the two components of the curvature of the reaction path: vibrational and angular. Recrossing time estimates depend on structural parameters only. Note, however, the role played by momenta: depending on their phase, the two components of potential energy can either cooperate and hasten recrossing or interfere and delay it.

TABLE I. Recrossing times for the 16 trajectories of a forward reaction studied at low energies. Initial conditions assuming energy equipartition defined in Eqs. (4.2)–(4.5). Fifth column: g or u parity.

Initial	conditions				Recrossing time	
$r_* + \delta r_*$	$\theta_* + \delta \theta_*$	$+p_{r_*}$	$+p_{\theta_*}$	g	$\langle \tau^{fwd} \rangle_0 - \Delta \tau^{vib} - \Delta \tau^{ang}$	Recrossing in the near future if the TS is soft
$r_* + \delta r_*$	$\theta_* + \delta \theta_*$	$+p_{r_*}$	$-p_{\theta_*}$	u	$\langle \tau^{fwd} \rangle_0 - \Delta \tau^{vib} + \Delta \tau^{ang}$	
$r_* + \delta r_*$	$\theta_* + \delta \theta_*$	$-p_{r_*}$	$+p_{\theta_*}$	u	$\langle \tau^{fwd} \rangle_0 + \Delta \tau^{vib} - \Delta \tau^{ang}$	
$r_* + \delta r_*$	$\theta_* + \delta \theta_*$	$-p_{r_*}$	$-p_{\theta_*}$	g	$\langle \tau^{fwd} \rangle_0 + \Delta \tau^{vib} + \Delta \tau^{ang}$	
$r_* - \delta r_*$	$\theta_* - \delta \theta_*$	$+p_{r_*}$	$+p_{\theta_*}$	g	$-\langle \tau^{fwd} \rangle_0 + \Delta \tau^{vib} + \Delta \tau^{ang}$	Recrossing in the recent past if the TS is soft
$r_* - \delta r_*$	$\theta_* - \delta \theta_*$	$+p_{r_*}$	$-p_{\theta_*}$	u	$-\langle \tau^{fwd} \rangle_0 + \Delta \tau^{vib} - \Delta \tau^{ang}$	
$r_* - \delta r_*$	$\theta_* - \delta \theta_*$	$-p_{r_*}$	$+p_{\theta_*}$	u	$-\langle \tau^{fwd} \rangle_0 - \Delta \tau^{vib} + \Delta \tau^{ang}$	
$r_* - \delta r_*$	$\theta_* - \delta \theta_*$	$-p_{r_*}$	$-p_{\theta_*}$	g	$-\langle \tau^{fwd} \rangle_0 - \Delta \tau^{vib} - \Delta \tau^{ang}$	
$r_* - \delta r_*$	$\theta_* + \delta \theta_*$	$+p_{r_*}$	$+p_{\theta_*}$	u	$\langle \tau^{fwd} \rangle_0 + \Delta \tau^{vib} - \Delta \tau^{ang}$	Recrossing in the near future if the TS is stiff
$r_* - \delta r_*$	$\theta_* + \delta \theta_*$	$+p_{r_*}$	$-p_{\theta_*}$	g	$\langle \tau^{fwd} \rangle_0 + \Delta \tau^{vib} + \Delta \tau^{ang}$	
$r_* - \delta r_*$	$\theta_* + \delta \theta_*$	$-p_{r_*}$	$+p_{\theta_*}$	g	$\langle \tau^{fwd} \rangle_0 - \Delta \tau^{vib} - \Delta \tau^{ang}$	
$r_* - \delta r_*$	$\theta_* + \delta \theta_*$	$-p_{r_*}$	$-p_{\theta_*}$	u	$\langle \tau^{fwd} \rangle_0 - \Delta \tau^{vib} + \Delta \tau^{ang}$	
$r_* + \delta r_*$	$\theta_* - \delta \theta_*$	$+p_{r_*}$	$+p_{\theta_*}$	u	$-\langle \tau^{fwd} \rangle_0 - \Delta \tau^{vib} + \Delta \tau^{ang}$	Recrossing in the recent past if the TS is stiff
$r_* + \delta r_*$	$\theta_* - \delta \theta_*$	$+p_{r_*}$	$-p_{\theta_*}$	g	$-\langle \tau^{fwd} \rangle_0 - \Delta \tau^{vib} - \Delta \tau^{ang}$	
$r_* + \delta r_*$	$\theta_* - \delta \theta_*$	$-p_{r_*}$	$+p_{\theta_*}$	g	$-\langle \tau^{fwd} \rangle_0 + \Delta \tau^{vib} + \Delta \tau^{ang}$	
$r_* + \delta r_*$	$\theta_* - \delta \theta_*$	$-p_{r_*}$	$-p_{\theta_*}$	u	$-\langle \tau^{fwd} \rangle_0 + \Delta \tau^{vib} - \Delta \tau^{ang}$	

The behavior of the remaining eight trajectories cannot be determined by the present methods. The reactive trajectories expected in TST are to be found among them. However, recrossings cannot be excluded. They are possible but uncertain. What can be said is that if they take place, then they must either occur in the distant future or have taken place in the remote past, i.e., far away from the saddle point. The decision to recross is then taken in a region located far away from the saddle where the parameterization adopted in Sec. III may become inadequate. Here, we are beyond the realm of TST, which postulates that the reaction rate is determined by the dynamics in a very small fraction of phase space. These remote past and distant future recrossings are termed global recrossings by Wiggins and co-workers:[22,23] "A global recrossing is a mechanism by which a trajectory that has left the neighborhood of the dividing surface crosses it again ... Global recrossings cannot be avoided, regardless of the choice of dividing surface." Explicit classical trajectory calculations that substantiate these views have been done by Garrett and Truhlar,[53] by Cho *et al.*,[54] and by Pritchard.[55]

VII. THE MICROCANONICAL ENSEMBLE

It is now highly desirable to move up from our bundle of 16 trajectories to a full-fledged microcanonical ensemble. Assuming microcanonical equilibrium at the saddle point as a result of its previous history in a strongly nonlinear force field is more realistic than taking energy equipartition for granted. For that purpose, energy is increased in one degree of freedom and decreased in another one to the same extent. This transfer can be done in a variety of ways, e.g., by replacing Eqs. (4.2)–(4.5) by

$$p_{r_*} = \sqrt{\frac{\mu}{M}} \, P_{R_*} \sqrt{1+\xi}, \tag{7.1}$$

$$\delta_{r_*} = \frac{P_{R_*}}{\sqrt{M\,\mu}\,\omega_*} \sqrt{1-\xi}, \tag{7.2}$$

$$p_{\theta_*} = \left(\frac{I}{M}\right)^{1/2} P_{R_*} \sqrt{1+\zeta}, \tag{7.3}$$

$$\delta\theta_* = \arcsin\left(\frac{P_{R_*}}{\sqrt{2\,M\,V_0}} \sqrt{1-\zeta}\right), \tag{7.4}$$

where the dimensionless parameters ξ and ζ are confined to the range $[-1, +1]$.

With this new set of initial conditions, the recrossing time of each individual trajectory, calculated from the cubic equation of motion as in Sec. V, is too complicated to be reported here. However, two interesting remarks, valid only at not too high energies, are appropriate.

First, considering, e.g., a soft TS, the eight trajectories having $\{r_* + \delta r_*, \theta_* + \delta\theta_*\}$ and $\{r_* - \delta r_*, \theta_* - \delta\theta_*\}$ as initial conditions all have recrossing times that, as before, are still given by the eight possible sign choices in Eq. (6.4), where each of the three terms $\langle\tau^{fwd}\rangle_0$, $\Delta\tau^{vib}$, and $\Delta\tau^{ang}$, is now a function of ξ and ζ.

Second, considering again a soft TS, a simpler expression is obtained for the doubly averaged recrossing time, i.e., first averaged over the four members of the set having $\{r_* + \delta r_*, \theta_* + \delta\theta_*\}$ as initial conditions, then over the parameters ξ and ζ in a symmetrical range. The broader the range, the more it deviates from the estimate valid under energy equipartition, given in Eq. (5.9). The maximum deviation is obtained after averaging over the maximum range $[-1, +1]$; it increases the average recrossing time by about 6% with respect to the value given in Eq. (5.9) in practically all cases.

Similar remarks can be made, with other initial conditions, if the TS is stiff.

Energy shifts other than those adopted in Eqs. (7.1)–(7.4) (e.g., shifting energy from the angular coordinate to the vibrational momentum, etc.) all lead to the same conclusion. This means that the average recrossing times derived in Secs. V and VI under the assumption of energy equipartition for the bundle of 16 trajectories are also valid for a microcanonical ensemble.

VIII. MOTION COORDINATION

We again come back to our bundle of 16 trajectories. Recall that they can be partitioned into two sets, *gerade* and *ungerade*. As shown in Paper I,[41] and as stated here in Eq. (2.7), these two sets are expected to have average equations of motion very close to each other. When the Hamiltonian is given by Eq. (2.1) and when initial conditions are given by Eqs. (4.2)–(4.5), Eq. (2.7) can be written explicitly:

$$\langle R(t)\rangle_g - \langle R(t)\rangle_u = 24\sqrt{2}\, \frac{P_{R_*}^4 \sqrt{I_*}}{M^3 \mu^2 R_* r_*^4 \omega_*}$$
$$\times \left(\sqrt{V_0} - \frac{\beta_{\theta\theta}}{\sqrt{V_0}}(1+\gamma r_*/2)\right) t^4 + \cdots. \tag{8.1}$$

Due to the heaviness of the nuclear masses, the difference between the two average trajectories can be expected to be quite small. This is even more so for the (more complicated) next term, which is quintic both in time and momentum. The hexic term is extremely complicated and starts with terms quartic in the translational momentum.

Similar relationships hold for the other degrees of freedom:

$$\langle r(t)\rangle_g - \langle r(t)\rangle_u = -32\sqrt{2}\frac{P_{R_*}^4 \sqrt{I_*} \sqrt{V_0}}{M^2 \mu^3 r_*^5 \omega_*}\, t^4 + \cdots, \tag{8.2}$$

$$\langle \theta(t)\rangle_g - \langle \theta(t)\rangle_u = -4\sqrt{2}\, \frac{P_{R_*}^4\, \gamma\, \beta_{r\theta}\, \sqrt{I_*}}{M^4\, \mu\, R_*^4\, \omega_*\, \sqrt{V_0}}\, t^4 + \cdots, \tag{8.3}$$

$$\langle P_R(t)\rangle_g - \langle P_R(t)\rangle_u = 96\sqrt{2}\, \frac{P_{R_*}^4 \sqrt{I_*}}{M^2 \mu^2 R_* r_*^4 \omega_*}$$
$$\times \left(\sqrt{V_0} - \frac{\beta_{\theta\theta}}{\sqrt{V_0}}(1+\gamma r_*/2)\right) t^3 + \cdots. \tag{8.4}$$

$$\langle R \rangle_g - R_* \,,\; \langle R \rangle_u - R_*$$
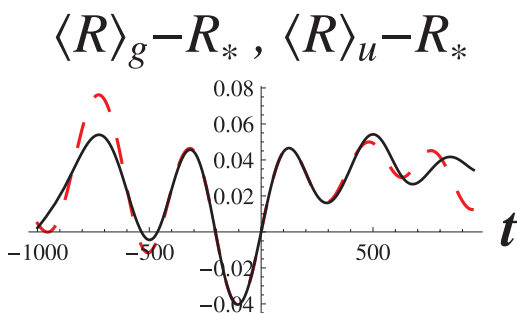

FIG. 2. Motion coordination among classical trajectories for the reaction HCO → H + CO calculated by numerical integration of Hamilton's canonical equations. Black solid line: Average of the set of *gerade* trajectories. Red dashed line: Average of the set of *ungerade* trajectories. Time and distances are in atomic units.

$$\langle p_r(t) \rangle_g - \langle p_r(t) \rangle_u = -128\sqrt{2}\,\frac{P_{R_*}^4\,\sqrt{I_*}\,\sqrt{V_0}}{M^2\,\mu^2\,r_*^5\,\omega_*}\,t^3 + \cdots,$$

(8.5)

$$\langle p_\theta(t) \rangle_g - \langle p_\theta(t) \rangle_u = 288\sqrt{2}\,\frac{P_{R_*}^5\,\sqrt{I_*}\,\theta_*\,\sqrt{V_0}}{M^3\,\mu^2\,R_*\,r_*^4\,\omega_*}\,t^4 + \cdots.$$

(8.6)

A numerical illustration of this coordination is given in Fig. 2.

When initial conditions depart from strict energy equipartition, the calculations are repeated with the energy partitioning described in Eqs. (7.1)–(7.4) and similar ones. The structure of Eqs. (8.1)–(8.6) is found to remain valid, except that their right-hand side is now multiplied by $(1 - \xi^2)^{1/2}(1 - \zeta^2)^{1/2}$. A further average transforms the latter expression into a coefficient whose numerical value is lower than one. Since

$$\frac{1}{2} \int_{-1}^{+1} \sqrt{1 - \xi^2}\, d\xi = \frac{\pi}{4},$$

the maximum lowering is seen to be equal to $(\pi/4)^2$, i.e., of the order of the order of 60%.

The smallness of the right-hand side of Eqs. (8.1)–(8.6), (which results from the presence of heavy nuclear masses in their denominators) indicates that *gerade* and *ungerade* trajectories coordinate their motions. This coordination is excellent in the vicinity of the saddle point but fades out at long (positive or negative) times, i.e., far away from the TS.

IX. CONCLUDING REMARKS

The recrossing times estimates given in Secs. V and VI have been derived from a series expansion in P_{R_*}, truncated to its lowest term, and thus are valid at low energies only. Note that they are expressed in terms of topographical features of the potential energy surface only. Thus, at short times and at not too high energies, essential dynamical features can be described quite simply and in terms of elementary local structural parameters only. The local nature of the needed information achieves the objectives of TST.

The expressions of the recrossing times (Eqs. (5.9), (5.13), (5.15), and (5.17)) all contain $\sqrt{M}\,R_*$ as a prefactor.

From Eq. (3.4), one deduces

$$\sqrt{M}\,R_* = \frac{6\sqrt{2}\,\Delta E}{\Omega}.$$

(9.1)

This relation accounts for the observation that, as noted by Berry *et al.*,[19,45] a low value of the imaginary frequency Ω is expected to induce long recrossing times and even, possibly, no recrossing at all. However, as argued in more recent work,[20,21] this is not the only factor that determines the "collimation"[19] of trajectories; the magnitude of the reverse activation energy barrier ΔE, together with the structural parameters μ, $r_* - r_\infty$, ω_*, θ_*, and V_0, also play a role. Moreover, at higher energies, the more complicated Eq. (5.10) must be used, in which the coupling elements β_{ij} of the three-body interaction term (Eq. (3.12)) appear.

Equation (6.3) (which is valid only in the cubic approximation) corresponds to a structuration of phase space in the neighborhood of the TS. The set of initial conditions corresponding to $R = R_*$ and to a prescribed value of P_{R_*} and of the total energy can be seen as a subspace of the total phase space. This subspace is structured in the sense that it contains points that can be defined as groups of eight, in such a way that the eight trajectories originating from them as initial conditions all have recrossing times that are given by the eight possible sign choices in an expression having the form

$$\tau_r = \pm\,\langle \tau \rangle_0 \pm \Delta\tau^{vib} \pm \Delta\tau^{ang},$$

where the subscript r is as an index that runs between 1 and 8.

By analogy with fluid mechanics, one might be tempted to term turbulent (and hence chaotic) that half of trajectories that recross close to the saddle point, and laminar (hence regular) the other half whose contingent recrossing is excluded in the TS region and shifted to distant future or remote past. However, this description is not appropriate because the initial conditions specified in Sec. IV are not separated by infinitesimal deviations. Chaos requires fast separation of trajectories for adjacent initial conditions. Hence, even the short-time recrossing trajectories must be termed regular. The local Liapunov exponent at the saddle point is zero for all trajectories. An accurate diagnostic test for chaotic behavior requires an analysis at a much finer mesh than what has been done here.

ACKNOWLEDGMENTS

[1]P. Pechukas, in *Dynamics of Molecular Collisions, Part B*, edited by W. H. Miller (Plenum, New York, 1976), p. 269.

[2]D. G. Truhlar, B. C. Garrett, and S. J. Klippenstein, J. Phys. Chem. **100**, 12771 (1996).

[3]A. Fernandez-Ramos, J. A. Miller, S. J. Klippenstein, and D. G. Truhlar, Chem. Rev. **106**, 4518 (2006).

[4]E. Wigner, Trans. Faraday Soc. **34**, 29 (1938).

[5]B. C. Garrett and D. G. Truhlar, in *Theory and Applications of Computational Chemistry: The First Forty Years*, edited by C. Dykstra, G. Frenking, K. S. Kim, and G. E. Scuseria (Elsevier, 2005), pp. 67–87.

[6]E. Pollak and P. Pechukas, J. Chem. Phys. **69**, 1218 (1978).

[7]M. J. Davis and S. K. Gray, J. Chem. Phys. **84**, 5389 (1986).

[8]E. R. Lovejoy, S. K. Kim, and C. B. Moore, Science **256**, 1541 (1992).

[9]S. K. Kim, E. R. Lovejoy, and C. B. Moore, J. Chem. Phys. **102**, 3202 (1995).

[10]R. A. Marcus, Science **256**, 1523 (1992).

[11]S. Y. Grebenshchikov, R. Schinke, and W. L. Hase, in *Comprehensive Chemical Kinetics, Vol. 39, Unimolecular Kinetics Part 1. The Reaction Step*, edited by N. J. B. Green (Elsevier, New York, 2003), pp. 105–242.

[12]W. L. Hase and R. Schinke, in *Theory and Applications of Computational Chemistry: The First Forty Years*, edited by C. Dykstra, G. Frenking, K. S. Kim, and G. E. Scuseria (Elsevier, New York, 2005), pp. 397–423.

[13]W. H. Miller, Faraday Discuss. Chem. Soc. **62**, 40 (1977).

[14]W. H. Miller, R. Hernandez, N. C. Handy, D. Jayatilaka, and A. Willets, Chem. Phys. Lett. **172**, 62 (1990).

[15]R. Hernandez and W. H. Miller, Chem. Phys. Lett. **214**, 129 (1993).

[16]S. Keshavamurthy and W. H. Miller, Chem. Phys. Lett. **205**, 96 (1993).

[17]D. J. Wales and R. S. Berry, J. Phys. B **24**, L351 (1991).

[18]R. J. Hinde, R. S. Berry, and D. J. Wales, J. Chem. Phys. **96**, 1376 (1992).

[19]R. J. Hinde and R. S. Berry, J. Chem. Phys. **99**, 2942 (1993).

[20]J. R. Green, T. S. Hofer, R. S. Berry, and D. J. Wales, J. Chem. Phys. **135**, 184307 (2011).

[21]J. R. Green, T. S. Hofer, D. J. Wales, and R. S. Berry, Mol. Phys. **110**, 1839 (2012).

[22]H. Waalkens, A. Burbanks, and S. Wiggins, J. Chem. Phys. **121**, 6207 (2004).

[23]H. Waalkens, R. Schubert, and S. Wiggins, Nonlinearity **21**, R1 (2008).

[24]A. Goussev, R. Schubert, H. Waalkens, and S. Wiggins, Adv. Quantum Chem. **60**, 269 (2010).

[25]T. Komatsuzaki and R. S. Berry, J. Chem. Phys. **110**, 9160 (1999).

[26]T. Komatsuzaki and R. S. Berry, Phys. Chem. Chem. Phys. **1**, 1387 (1999).

[27]T. Komatsuzaki and R. S. Berry, J. Mol. Struct.: THEOCHEM **506**, 55 (2000).

[28]T. Komatsuzaki and R. S. Berry, Proc. Natl. Acad. Sci. U.S.A. **98**, 7666 (2001).

[29]T. Komatsuzaki and R. S. Berry, J. Phys. Chem. A **106**, 10945 (2002).

[30]T. Komatsuzaki and R. S. Berry, Adv. Chem. Phys. **123**, 79 (2002).

[31]S. Kawai and T. Komatsuzaki, Phys. Rev. Lett. **105**, 048304 (2010).

[32]C. B. Li, Y. Matsunaga, M. Toda, and T. Komatsuzaki, J. Chem. Phys. **123**, 184301 (2005).

[33]C. B. Li, A. Shoujiguchi, M. Toda, and T. Komatsuzaki, Phys. Rev. Lett. **97**, 028302 (2006).

[34]D. J. Wales, *Energy Landscapes* (Cambridge University Press, Cambridge, 2003).

[35]D. J. Wales, Philos. Trans. R. Soc., A **370**, 2877 (2012).

[36]A. O. Cohen and R. A. Marcus, J. Chem. Phys. **49**, 4509 (1968).

[37]W. H. Miller, J. Chem. Phys. **53**, 1949 (1970).

[38]W. H. Miller, J. Chem. Phys. **54**, 5386 (1971).

[39]S. C. Farantos and J. Tennyson, J. Chem. Phys. **84**, 6210 (1986).

[40]N. Smith, J. Chem. Phys. **85**, 1987 (1986).

[41]J. C. Lorquet, J. Chem. Phys. **140**, 134303 (2014).

[42]H. Goldstein, C. Poole, and J. Safko, *Classical Mechanics* (Addison Wesley, San Francisco, 2002).

[43]K. S. Sorbie and J. N. Murrell, Mol. Phys. **29**, 1387 (1975).

[44]J. N. Murrell, S. Carter, S. C. Farandos, P. Huxley, and A. J. C. Varandas, *Molecular Potential Energy Functions* (Wiley, Chichester, 1984).

[45]J. C. Lorquet, J. Phys. Chem. A **115**, 4610 (2011).

[46]G. Simons, R. G. Parr, and J. M. Finlan, J. Chem. Phys. **59**, 3229 (1973).

[47]H. Eyring, J. Walter, and G. E. Kimball, *Quantum Chemistry* (Wiley, New York, 1944).

[48]U. Lourderaj and W. L. Hase, J. Phys. Chem. A **113**, 2236 (2009).

[49]S. J. Klippenstein, Y. Georgievski, and L. B. Harding, J. Phys. Chem. A **115**, 14370 (2011).

[50]L. B. Harding, S. J. Klippenstein, and A. W. Jasper, J. Phys. Chem. A **116**, 6967 (2012).

[51]J. M. Bowman and B. C. Shepler, Annu. Rev. Phys. Chem. **62**, 531 (2011).

[52]S. W. Cho, W. L. Hase, and K. N. Swamy, J. Phys. Chem. **94**, 7371 (1990).

[53]B. C. Garrett and D. G. Truhlar, J. Phys. Chem. **84**, 805 (1980).

[54]Y. J. Cho, S. R. V. Linde, L. Zhu, and W. L. Hase, J. Chem. Phys. **96**, 8275 (1992).

[55]H. O. Pritchard, J. Phys. Chem. A **109**, 1400 (2005).